arXiv:1404.5075v1 [cond-mat.quant-gas] 20 Apr 2014

Solitons in a hard-core bosonic system: Gross-Pitaevskii type and beyond

Radha Balakrishnan[1] and Indubala I Satija[2]
[1] *The Institute of Mathematical Sciences, Chennai 600113, India and*
[2] *School of Physics, Astronomy and Computational Sciences, George Mason University, Fairfax, VA 22030, USA*

A unified formulation that obtains solitary waves for various background densities in the Bose-Einstein condensate of a system of hard-core bosons with nearest neighbor attractive interactions is presented. In general, two species of solitons appear: A nonpersistent (NP) type that fully delocalizes at its maximum speed, and a persistent (P) type that survives even at its maximum speed, and transforms into a periodic train of solitons above this speed. When the background condensate density is nonzero, both species coexist, the soliton is associated with a constant intrinsic frequency, and its maximum speed is the speed of sound. In contrast, when the background condensate density is zero, the system has neither a fixed frequency, nor a speed of sound. Here, the maximum soliton speed depends on the frequency, which can be tuned to lead to a cross-over between the NP-type and the P-type at a certain critical frequency, determined by the energy parameters of the system. We provide a single functional form for the soliton profile, from which diverse characteristics for various background densities can be obtained. Using the mapping to spin systems enables us to characterize the corresponding class of magnetic solitons in Heisenberg spin chains with different types of anisotropy, in a unified fashion.

PACS numbers: 03.75.Ss, 03.75.Mn, 42.50.Lc, 73.43.Nq

I. INTRODUCTION

Experimental demonstration [1–6] of solitary waves/solitons [7] in Bose-Einstein condensates (BEC)[8, 9] is one of the hallmarks of quantum coherence inherent in ultracold atomic systems As predicted theoretically in the Gross-Pitaevskii equation (GPE) [9], which describes *weakly interacting* bosons in the mean field approximation, a condensate of Rb atoms with repulsive interactions was found to support dark solitary waves (density depressions) [1], while a Li condensate [2] with attractive interactions supported bright solitary waves (density elevations)[10]. Various recent theoretical studies [11] have investigated soliton evolution in quantum many body systems to understand the role of quantum fluctuations on mean field solutions. Intrinsically nonlinear, the BEC systems continue to remain an active area to explore the presence of nonlinear localized modes. In view of the fact that GPE also describes nonlinear optical systems, these studies are relevant beyond the BEC literature.

In our previous work [12] , we investigated the propagation of solitonic excitations in a system of hard-core bosons (HCB), which describes *strongly repulsive* bosons. By mapping an extended Bose-Hubbard model [13] for hard-core bosons on a lattice, with nearest neighbor (nn) hopping energy t and (nn) interactions V to a spin model, we used spin-coherent states [14] to obtain the condensate density for HCB as $\rho^s = \rho(1-\rho)$, where ρ is the bosonic (particle) density for the HCB system. We derived the continuum evolution equation for the condensate wave function, which we called HGPE, 'H' standing for HCB. The only model-dependent effective energy parameter that appears in HGPE is $E_e = (t-V)/t$.

For the case $E_e > 0$, we analyzed unidirectional solitary wave excitations in HGPE when the background density ρ_0 contains *both particles and holes*, For a hard-core system, this implies $0 < \rho_0 < 1$. We refer to this as the 'fractional filling' case. This corresponds to a non-zero condensate density ρ_0^s in the background. Under these conditions, the system was shown to possess an intrinsic speed of sound and an intrinsic frequency parameter. These are *fixed* in the sense that they depend on the given background density and the system parameters. This frequency can be shown to be just the frequency associated with the phase of the homogeneous condensate in the background.

At half-filling, both bright and dark solitons which are mirror images of each other are supported for the density ρ. Further, both are *nonpersistent* (NP) type solitons that flatten out and delocalize at their maximum speed, which is the speed of sound in the system. Intriguingly, for half-filling, the behavior of solitons for the condensate density ρ^s in this strongly repulsive system can be shown to be [15] very similar to that of the GP soliton in a weakly repulsive system, since it is dark, and delocalizes at sonic speed.

Away from half-filling, we found *two distinct species* of solitons that coexist in the HCB system. For $0 < \rho_0 < 1/2$ $(1 > \rho_0 > 1/2)$, one is a NP-type dark (bright) soliton for density, that delocalizes completely at the speed of sound, while the other is a novel *persistent* P-type bright (dark) soliton that survives as a localized entity, even at its maximum speed, In addition, the P-soliton transforms into a train of solitons at supersonic speeds, quite unlike a GP soliton. The corresponding condensate density soliton for the NP-type is always dark, while that for the P-type not only survives at the speed of sound, but also becomes completely bright at this speed [12]. This brightness is quite unexpected in a very strongly repulsive system like the HCB. Preliminary results on collision of these solitary waves [16] show that they emerge unscathed, suggesting that they could be strict solitons. Additionally, in a recent study [17], we have also shown that both the above species of solitary waves remain stable on the lattice under time evolution, and also survive quantum fluctuations, for experimentally accessible time scales.

A natural question that arises is whether the HCB system can support solitary wave excitations for $E_e > 0$, when the background density has *only* particles or *only* holes, i.e., for $\rho_0 = 1$ or $\rho_0 = 0$. We shall refer to this as the "integer filling

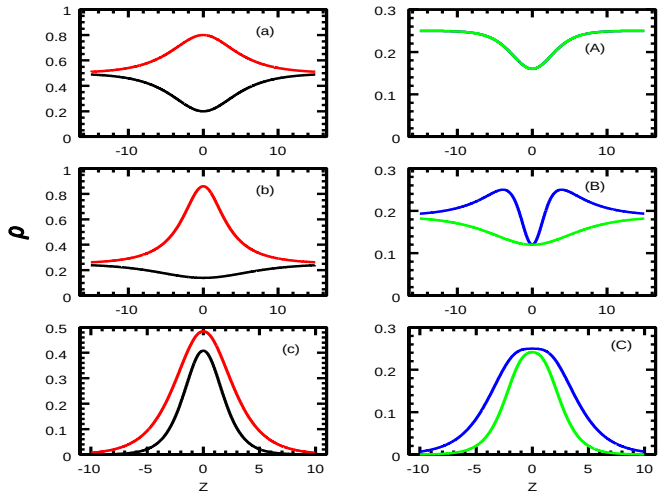

FIG. 1: (color on line) Solitary waves with background density $\rho_0 = 0.5$ (a), $\rho_0 = 0.25$ (b), and $\rho_0 = 0$ (c) for fixed $E_e = 0.1$ and $v/c = 0.8$. Here red and black show the persistent (P-type) and non-persistent (NP-type) solitons. (A), (B) and (C) show the corresponding condensate density ρ^s, where the blue and the green respectively correspond to P and NP-type, respectively. For $\rho_0 = 0.5$, the plots for ρ^s for the two types overlay each other. For $\rho_0 = 0$ which exhibits only bright solitons, the P and the NP types plotted correspond to $E_\omega = 0.15$ and 0.3 respectively.

" case. This corresponds to a vanishing condensate density in the background. This represents a distinct class in contrast to the fractional filling case, because this system has neither an intrinsic speed of sound to limit the soliton speed, nor a fixed intrinsic frequency. In addition, it is also worth exploring the existence of solitons for $E_e \leq 0$.

In this paper, we address above questions within a *unified formulation* that obtains a single functional form for the density soliton which is valid for *both* fractional filling and integer filling background densities, as well as for $E_e > 0$ and $E_e \leq 0$. Using this, we can obtain the diverse characteristics of solitons for the various possible cases. We find that for integer filling, the soliton is characterized both by its speed and by its independently tunable frequency parameter. This is unlike the fractional filling case [12], when it is characterized only by its speed. Interestingly, maximum soliton speed is seen to depend on this frequency ω. leading to two competing energy scales, $E_\omega = \hbar\omega/t$ and the effective energy E_e.

For $E_e > 0$, integer fillings, while both NP and P-type solitons appear, they do not coexist. Depending upon the relative strength of E_ω and E_e, the system supports either a P -soliton that persists at its (frequency-dependent) maximum speed or a NP- soliton which delocalizes at this speed. Thus the frequency can be *tuned* to lead to a cross-over between the NP-type and the P-type soliton at a certain *critical frequency*, determined by E_e.

For $E_e \leq 0$, we show that while only NP-solitons are supported for integer fillings, *no* soliton solutions exist for fractional filling backgrounds.

One general interesting feature of HCB solitons for the integer-filling background (for all E_e) is that unlike the fractional-filling case where the maximum soliton speed is limited by the speed of sound, high-speed solitons are possible here, since the maximum soliton speed is controlled by the tunable frequency.

Finally, using the mapping of HCB to spins, the single functional form we obtain for the density soliton also enables us to classify the characteristics of magnetic solitons in the isotropic Heisenberg spin chain as well as the easy-plane and easy-axis anisotropic spin chains, in a unified fashion.

II. THE EXTENDED BOSE-HUBBARD MODEL

A. The Model

As is well known, by loading ultracold bose atoms on to an optical lattice [18] which is created using standing waves of laser light, it has become possible to realize various models of condensed matter systems, in the cold atoms lab. More important, it is also possible to create lattices of different dimensions, as well as *tune* the value of the parameters in the model, experimentally. This motivates us to consider the following Hamiltonian for the extended Bose-Hubbard (BH) model [13] in d dimensions:

$$H = -\sum_{j,a}[t\,(b_j^\dagger b_{j+a} + h.c.) + V n_j n_{j+a}] + \sum_j \left[U n_j(n_j - 1) + 2t n_j\right], \tag{1}$$

where $b_j^\dagger$ (b_j) are the normal boson creation (annihilation) operators, which satisfy the usual commutation relations $[b_j, b_l^\dagger] = \delta_{jl}$ and $[b_j, n_l] = b_j\delta_{jl}$, where n_j is the number operator at site j. a labels nearest-neighbor (nn) sites, t is the nn hopping parameter, U denotes the on-site repulsive energy and V is the nn interaction. The on-site term $2tn_j$ has been added

so as to obtain the correct kinetic energy term in the continuum version of the many-body bosonic Hamiltonian, which will also enable direct comparison with the usual form of the GPE.

While several aspects of model (1), such as quantum phase transitions, phase diagrams, etc. have been studied [13], our interest here is to investigate whether this model can support nonlinear dynamical excitations like solitons.

B. BEC evolution for weakly repulsive normal bosons and GPE: Order parameter evolution using bosonic coherent states

Before proceeding to the BEC of strongly repulsive bosons, it is instructive to study the BH model for normal bosons and its connection to GPE. The usual BH model contains only the on-site *finite* repulsion term U and no nn interaction term V in Eq. (1). The order parameter of a BEC is conventionally defined as the expectation value of the boson annihilation operator. It has been argued [19] that the Glauber (or bosonic) coherent- state representation may be appropriate for computing the expectation value, since it is well known that coherent states are most useful in the context of quantum many-body systems which display quantum effects in macroscopic scales as in a BEC.

Writing down operator evolution equation of b_j using $i\hbar(db_j/d\tau) = [b_j, H]$ where H is the usual BH model, and τ stands for time, the boson coherent state expectation value of the above operator equation yields the order parameter evolution. Its continuum version can be shown to be identical in form to the following Gross-Pitaevskii equation (GPE) [9] for the time evolution of the BEC order parameter for weakly interacting bosons:

$$i\hbar\psi_\tau + \frac{\hbar^2}{2m}\nabla^2\psi - g|\psi|^2\psi = 0, \tag{2}$$

where we have identified the hopping parameter $ta^2 = \hbar^2/m$ and $U = g = 4\pi\hbar^2\bar{a}/m$. (Here $\bar{a}$ is the s-wave scattering length in an ultracold dilute bose gas with local (weak) interaction $g = U$). Since $U > 0$ in Eq. (1), Eq. (2) describes the condensate dynamics for weak repulsive interaction between bosons. It is to be noted that the use of boson coherent state expectation values leads to a mean field description, so that for the GPE, the condensate density ρ^s is equal to the particle density ρ.

Although soliton solutions of GPE are well known, our analysis presented below differs from those discussed in the BEC soliton literature [9, 10]. As we shall see, our systematic methodology for obtaining solitons in this weakly repulsive GPE will also be useful in arriving at a unified formulation for finding soliton solutions for BEC in the strongly repulsive system described by hard-core bosons, for various background densities.

It is well known that linear modes of the GPE can be found by analyzing small amplitude traveling wave solutions of Eq. (2) to yield the Bogoliubov dispersion relation [9], which shows that the modes are sound waves with speed $c_g = \sqrt{\frac{g\rho_0}{m}}$. In order to study solitary waves in the x-direction, we first set $\psi = \sqrt{\rho(x,\tau)}\exp i\phi(x,\tau)$ in Eq. (2), and separate its real and imaginary parts to obtain coupled equations for ρ and ϕ. To study soliton propagation, typically one looks for unidirectional traveling wave solutions of the form

$$\rho(x,\tau) = \rho_0 + f(z); \;\; \phi(x,\tau) = \omega\tau + \phi(z), \tag{3}$$

where $z = (x - v\tau)$. Here, v is the speed of the traveling wave and ω is a frequency parameter.

Using Eqs. (3) in the coupled equations for ρ and ϕ obtained from Eq. (2), a lengthy but straightforward calculation yields

$$-v\rho_z + \frac{\hbar}{m}\frac{d}{dz}(\rho\phi_z) = 0 \tag{4}$$

$$-4\hbar\rho^2\omega + 4\hbar\rho^2 v\phi_z + (\hbar^2/m)\rho\rho_{zz} - (\hbar^2/2m)\rho_z^2 - (2\hbar^2/m)\rho^2\phi_z^2 - 4g\rho^3 = 0 \tag{5}$$

where the subscript z stands for derivative with respect to z.

We are interested in soliton solutions with boundary conditions $\rho(z) \to \rho_0$ and the derivative $\phi_z \to 0$, as $|z| \to \infty$. With this, Eq. (4) can be easily integrated to yield

$$\phi_z = \frac{mv}{\hbar}\frac{(\rho - \rho_0)}{\rho}. \tag{6}$$

Substituting ϕ_z from (6) into Eq. (5), multiplying by $\rho_z\ \rho^-2$ and collecting terms appropriately, it becomes possible to integrate the resulting equation to yield

$$\frac{\hbar^2}{2m}\rho_z^2 = 2g\rho^3 - (2mv^2 - 4\hbar\omega)\rho^2 - \lambda_g\rho - 2mv^2\rho_0^2, \tag{7}$$

where λ_g is a constant of integration to be determined consistently. The subscript g is used to indicate that the quantity concerned corresponds to the GPE case.

Note that the right hand side of the above equation is a cubic polynomial. Since we are interested in finding localized solutions for $\rho(z)$, with the asymptotic boundary condition $(d\rho/dz) = 0$ as $\rho \to \rho_0$, we can write Eq. (7) in the form

$$\frac{\hbar^2}{2m}\rho_z^2 = (\rho-\rho_0)^2[M_g\rho + N_g]. \quad (8)$$

The unknown quantities M_g, N_g and λ_g are found by equating the right hand sides of Eqs. (7) and Eq. (8). For $\rho_o \neq 0$, we obtain $M_g = 2g;\ N_g = -2mv^2;\ \lambda_g = -2\rho_0[g\rho_0 + 2mv^2]$, along with

$$\omega = \omega_g = -g\rho_0/\hbar. \quad (9)$$

Thus the frequency ω that appears in Eq. (3) is a constant for the GP soliton.
Looking for solutions of the form

$$\rho(z) = \rho_0 + f(z), \quad (10)$$

and substituting for the expressions for M_g and N_g into Eq. (8), we get

$$\frac{\hbar}{2m}\frac{df}{dz} = \pm f[\frac{fg}{m} + c_g^2\gamma_g^2] \quad (11)$$

where $c_g = \sqrt{g\rho_0/m}$ is the Bogoliubov speed of sound we found earlier (see above (3), and $\gamma_g^2 = 1 - v^2/c_g^2$. Equation (11) can be integrated to give

$$f(z) = -\rho_0\,\gamma_g^2\,\mathrm{sech}^2(\mathrm{m}/\hbar)\gamma_\mathrm{g}\mathrm{c_g z}, \quad (12)$$

yielding the well-known GP dark soliton solution

$$\rho(z) = \rho_0[1 - \gamma_g^2\,\mathrm{sech}^2(\mathrm{m}/\hbar)\gamma_\mathrm{g}\mathrm{c_g z}]. \quad (13)$$

This is a dark soliton that describes a depression in the background density ρ_0. Its profile flattens out as v tends to the speed of sound c_g. *Thus the GP- dark soliton is of NP-type.*

The phase of the soliton is obtained by substituting Eq. (13) into Eq. (6) and integrating it to give $\phi(z) = -\tan^{-1}[(\gamma_g c_g/v)\tanh\gamma_g c_g z]$. This yields the phase jump across the soliton to be $\Delta\phi = -2\cos^{-1}[\frac{v}{c_g}]$.

It is important to note that while we looked for solutions for ρ and ϕ as in (3) that had two parameters v and ω, Eq. (9) shows that for the GP soliton, frequency $\omega = \omega_g = -g\rho_0/\hbar$ is not a variable parameter, but is determined by the local repulsion energy g and the background condensate density ρ_0. Thus the GP soliton has only a single variable parameter, its speed v which cannot exceed the speed of sound.

Further, an inspection of Eq. (2) shows that ω_g is has its origin in the purely time-dependent phase $\phi = \omega_g\tau$ associated with the background condensate density ρ_0, which is nonzero for the GP soliton. In other words, $\hbar\omega_g$ can be regarded as the energy of the background.

Finally, it is instructive to write f in terms of the BH model parameters by setting $\hbar = m = 1$ and $g = U$, with U denoting a dimensionless variable (U/t) :

$$f(z) = -\frac{c_g^2\gamma_g^2}{U[\cosh 2\gamma_g c_g z + 1]} \quad (14)$$

,

III. BEC EVOLUTION FOR STRONGLY REPULSIVE BOSONS AND HGPE: ORDER PARAMETER EVOLUTION USING SPIN-COHERENT STATES

We are interested in studying the condensate of a strongly repulsive boson system, described by the hard core boson limit $U \to \infty$. Firstly, we note that if we set the repulsion $U \to \infty$, then since $c_g^2 \to U \to \infty$ and $\gamma_g \to 1$, the GP soliton (14) found from the usual BH model flattens out and delocalizes. As we shall see, the addition of a nn attraction V as in the extended BH model (1) helps in localizing the soliton in the HCB system.

A. HCB system : Mapping to Spin- $\frac{1}{2}$ Hamiltonian

The limit $U \to \infty$ in the Hamiltonian (1) implies that two bosons cannot occupy the same site. i.e., boson operators anticommute at same site but commute at different sites. This leads to $b_j^2 = 0\,;\, n_j^2 = n_j\,;\, \{b_j,\, b_j^\dagger\} = 1\ ;\ [b_j,\, b_l^\dagger] = (1-2n_j)\delta_{jl}$. Identifying b_j = S_j^+ (spin-raising operator) and $n_j = \frac{1}{2} - S_j^z$ (operator for z-component of spin) yields the spin-$\frac{1}{2}$ algebra: $[S_j^+,\, S_l^-] = 2S_j^z\,\delta_{jl}$. Using the above identification to spin operators, the extended Bose-Hubbard Hamiltonian (1) for HCB maps to the following quantum XXZ Heisenberg spin-$\frac{1}{2}$ ferromagnetic (since $t > 0$) Hamiltonian in a magnetic field along the z-axis:

$$H_S = -\sum_{j,a}[t\,(S_j^+ S_{j+a}^- + h.c) + V S_j^z S_{j+a}^z] - \sum_j((t-V)d)S_j^z. \quad (15)$$

B. Order parameter evolution for the HCB system: HGPE

The dynamics of the HCB system is given by the Heisenberg equation of motion:

$$i\hbar\dot{S}_j^+ = [S_j^+, H_S] = (t-V)d\ \ S_j^+ - tS_j^z\sum_a S_{j+a}^+ + VS_j^+\sum_a S_{j+a}^z. \quad (16)$$

Since the condensate order parameter is the expectation value of the boson operator in a system, it is easy to see that for the hard-core boson system it becomes η_j, the expectation value

of the spin-flip operator , i.e., $\eta_j = \langle S_j^+ \rangle$.

We use spin-coherent states [14] as the natural choice for computing the above expectation value, due to the inherent coherence in the condensed phase of the HCB system [12]. This is analogous to the use of boson coherent states for defining the order parameter of a *weakly repulsive* system of normal bosons, which leads to the GPE, as we saw above.

The spin coherent state at a lattice site l is defined by $|\tau_l\rangle = (1 + |\tau_l|^2) \ \exp \ [\tau_l \, S_l^-] \ |0\rangle$, where $S_l^- = S_l^x - iS_l^y$ is the spin lowering operator, τ_l is a complex quantity, and $S_l^z|S\rangle = S|0\rangle$. For N spins, we work with the direct product $|\tau\rangle = \Pi_l^N |\tau_l\rangle$. The states $|\tau_l\rangle$ are normalized, nonorthogonal and over complete. It can be shown that the diagonal matrix elements of *single* spin operators in the spin coherent representation are identical to the corresponding expressions for a classical spin [14]. For $S = \frac{1}{2}$, it can be shown that the condensate number density $\rho_j^s = |\eta_j|^2$ and the particle number density $\rho_j = \langle n_j \rangle$ are related by [12]

$$\rho_j^s = \rho_j(1 - \rho_j) = \rho_j \ \rho_j^h, \tag{17}$$

where $\rho_j^h = (1 - \rho_j)$ is the hole density. Hence both particles and holes play equally important roles in determining the condensate properties. Further, in contrast to the GPE case, $\rho^s \neq \rho$, implying the presence of depletion in the HCB system.

As explained in [12], taking the spin coherent state expectation value of Eq. (16) leads to the evolution equation for the order parameter $\eta_j =< S_j^+ >$ on the lattice. A continuum description of the discrete equations is useful when the order parameter is a smoothly varying function with a length scale greater than the lattice spacing a. Using appropriate Taylor expansions for the various quantities appearing in the lattice equations [12] , we get

$$i\hbar \frac{\partial \eta}{d\tau} = -\frac{ta^2}{2}(1-2\rho) \ \nabla^2\eta - Va^2 \ \nabla^2\rho \ \ \eta + 2(t-V)d \ \rho \ \eta, \tag{18}$$

where τ stands for time and d is the dimensionality of the lattice. We call this equation HGPE, "H" representing HCB. Note that in Eq. (18), the condensate wave function is given by

$$\eta(\mathbf{r},\tau) = \sqrt{\rho^s(\mathbf{r},\tau)}\exp(i\phi(\mathbf{r},\tau)) = \sqrt{\rho(\mathbf{r},\tau)(1-\rho(\mathbf{r},\tau))}\exp(i\phi(\mathbf{r},\tau)), \tag{19}$$

where we have used Eq. (17). Substituting Eq. (19) into Eq. (18), coupled nonlinear evolution equations for the particle density ρ and the phase ϕ can be written down. From their solution, the condensate density $\rho_s = \rho(1 - \rho)$ as well as the condensate wave function η can be found.

While our discussion so far is for d-dimensions, our interest in this paper is to investigate solitons in a BEC trapped in a one-dimensional lattice/ highly anisotropic, cigar-shaped trap [10]. Therefore in what follows, we will set $d = 1$, and look for unidirectional traveling wave solutions.

IV. SOME GENERAL FEATURES OF HGPE

Before proceeding to our analysis of soliton solutions of HGPE, we point out some *general* features of the condensate parameter evolution of the HCB system as described by HGPE (Eq. (18). These will be useful in understanding the various characteristics of the soliton solutions we will find for this system.

A. GPE as a certain low-density approximation to HGPE

From Eq. (17), we note that in the low density approximation, we can set $\rho^s \approx \rho$. Using this in Eq. (19), we have, $\eta \to \psi = \sqrt{\rho}\exp i\phi$. In addition, if we also *neglect* nonlinear terms involving $\rho \ \nabla^2\eta$ and $\nabla^2\rho \ \eta$ in Eq. (18), we get the GPE given in Eq. (2), but with the identification $ta^2 = \hbar^2/m$, and with $2(t - V)$ as an effective local interaction between the (hard-core) bosons in the GPE limit. While in Eq. (2) obtained from the condensate dynamics of the usual BH model with normal bosons is always repulsive ($g > 0$), $2(t - V)$ arising as an approximation to the condensate dynamics of the extended BH model for HCB can be positive, negative or zero. However, by comparison with GPE discussion of c_g, the sound speed will be given by $\sqrt{2(t - V)\rho_0/m}$, for the approximated HGPE under consideration . Hence, only for $(t - V) > 0$, will there be a speed of sound for this limit.

B. Particle-hole symmetry

In the HGPE (Eq. (18)), if we set $(1-2\rho) = (\rho_h - \rho)$; $\rho = [1 + (\rho - \rho_h)]/2$, we get

$$i\hbar\,\frac{\partial\eta}{\partial\tau} = -\frac{ta^2}{2}(\rho_h-\rho)\ \eta_{xx} - \frac{V}{2}a^2\ (\rho-\rho_h)_{xx}\ \eta + (t-V)\,(\rho-\rho_h)\ \eta + \ (t-V)\eta \tag{20}$$

We may use the gauge transformation to remove the last term in Eq. (20)

$$\eta \to \eta \exp -i(t-V))\tau/\hbar, \tag{21}$$

$$i\hbar\,\frac{\partial\eta}{\partial\tau} = -\frac{ta^2}{2}(\rho_h-\rho)\ \eta_{xx} - \frac{V}{2}a^2\ (\rho-\rho_h)_{xx}\ \eta + (t-V)\,(\rho-\rho_h)\ \eta \tag{22}$$

In the above equation, we observe that interchanging the particle density ρ and the hole density ρ_h changes the overall sign of the right hand side. Also, η remains invariant under this interchange. This shows that if η is the wave function for the condensate of particles, η^* becomes the wave function for the condensate of holes. Thus Eq. (22) has a particle-hole symmetry and proves to be convenient for obtaining a unified formulation of the HCB condensate dynamics that we seek. Rewriting Eq. (22) in terms of ρ alone, we obtain

$$i\hbar\,\frac{\partial\eta}{\partial\tau} = -\frac{ta^2}{2}(1-2\rho)\ \eta_{xx} - Va^2\ \rho_{xx}\ \eta + (t-V)\,(2\rho-1)\ \eta. \tag{23}$$

C. Fractional filling and integer filling background densities: Differences in physical characteristics

One usually looks for solutions for the condensate that are spatially homogeneous asymptotically,i.e., $\rho \to \rho_0$, $\eta \to \sqrt{\rho_0(1-\rho_0)}\exp(i\phi_{\pm\infty})$. On substituting this asymptotic solution into Eq. (23), we find that for fractional filling backgrounds $0 < \rho_0 < 1$ for which the condensate background density is nonzero asymptotically, the phase must have a purely time dependent term $\omega_F\tau$ as well, with intrinsic frequency determined in terms of system parameters as $\hbar\omega_F/t = E_e[1-2\rho_0]/\hbar$, where E_e is a dimensionless effective energy parameter

$$E_e = \frac{t-V}{t}, \tag{24}$$

and the subscript F denotes fractional filling. In contrast, for the integer filling background with $\rho_0 = 0$ or 1 which implies a vanishing condensate density, Eq. (23) is identically satisfied asymptotically, and hence the frequency ω does not get determined, and remains a variable parameter.

Secondly, linear excitations of the HGPE analyzed using small amplitude solutions of Eq. (18) yields the speed of sound in the HCB condensate as [12]

$$c \sim \sqrt{2E_e\rho_0(1-\rho_0)}, \tag{25}$$

This implies that while there are sound wave modes for the fractional filling background when $E_e > 0$, they are absent for the integer filling case. For $E_e \leq 0$, the HCB system does not support sound waves for any filling.

Consistent with the above observations, we will indeed find that soliton solutions with fractional filling and integer filling background densities belong to two distinct classes, with only the former getting associated with a fixed frequency ω_F given earlier in this subsection, and a speed of sound as in Eq. (25).

V. SOLITON SOLUTIONS FOR THE HGPE

Setting $\eta = \rho(1-\rho)$ in Eq. (23) and equating real and imaginary parts, we obtain the following coupled equations for ρ and ϕ:

$$\hbar\rho_\tau/t = -a^2[\rho(1-\rho)\phi_x]_x \tag{26}$$

$$\hbar\phi_\tau/t = E_e(1-2\rho) + \frac{a^2}{4}\big[\frac{\rho_{xx}}{\rho(1-\rho)} - \frac{(1-2\rho)\rho_x^2}{2\rho^2(1-\rho)^2}\big] - E_e a^2\rho_{xx} - \frac{a^2}{2}(1-2\rho)\phi_x^2 \tag{27}$$

A. Exact nonlinear plane wave solutions

Although our interest is in finding soliton solutions which are localized in space, it is interesting to note that the above coupled nonlinear PDEs have *exact* plane wave solutions.

Taking $\rho(x,\tau) = \rho_0$, Eq. (26) gives $\phi_{xx} = 0$. This leads to plane wave solutions $\phi(x,\tau) = -kx + \Omega\tau$. Using this in Eq. (27), we get the exact dispersion relation for the plane waves, quadratic in k :

$$\hbar\Omega(k)/t = (\hbar\omega_F/t) - (\frac{1}{2} - \rho_0)a^2k^2 \tag{28}$$

where ω_F is the same as that found in the previous section. Thus for $\rho_0 > \frac{1}{2}$, the plane wave excitation is like a particle, whereas for $\rho_0 < \frac{1}{2}$ it is hole-like. For $\rho_0 = \frac{1}{2}$, $\Omega(k)$ vanishes, showing that the plane wave becomes static.

B. Solitons for fractional and integer filling background : A unified formulation

While the methodology that we will use to find solitary wave solutions of HGPE will be in close parallel with that of the GPE discussed in the last section, HGPE will be seen to support both bright and dark solitons, in contrast to the GPE which has only dark solitons. This essentially arises due to a particle-hole symmetry in the HCB model.

Looking for unidirectional traveling waves of the typical form (3), Eqs. (26) and (27) become

$$v\rho_z = \left[\rho(1-\rho)\phi_z\right]_z \tag{29}$$

and

$$[E_\omega - v\phi_z]\rho_z = E_e(1-2\rho)\rho_z + \frac{1}{8}\frac{d}{dz}[\frac{\rho_z^2}{\rho(1-\rho)}] - E_e\rho_{zz}\rho_z - \frac{1}{2}(1-2\rho)\phi_z^2\rho_z \tag{30}$$

where $v\hbar/at$ has now been defined as a dimensionless speed v. E_ω is a dimensionless energy (in units of hopping energy t) defined by

$$E_\omega = \frac{\hbar\omega}{t}, \tag{31}$$

Using boundary conditions $\rho \to \rho_0$ and $\phi_z \to 0$ as $|z| \to \infty$, Eq. (29) can be easily integrated to give

$$\phi_z = \frac{v(\rho-\rho_0)}{\rho(1-\rho)}, \tag{32}$$

Substituting Eq. (32) in Eq. (30) and integrating, we get the following general nonlinear ordinary differential equation valid for all values of E_e and background densities ρ_0:

$$\frac{1}{4}(d\rho/dz)^2\left[1 - 4E_e\rho(1-\rho)\right] = [-\rho_0^2v^2 + (2\rho_0-1)v^2 - \lambda_0]\rho + [2(E_e - E_\omega) - \lambda_0]\rho^2 + 2(2E_e - E_\omega)\rho^3 - 2E_e\rho^4] \tag{33}$$

where λ_0 is an integration constant. It is interesting to note the natural appearance of the two energies E_ω and E_e, associated with the frequency parameter ω in the phase ϕ, and an effective energy parameter $(t - V)$ in the BH model for HCB, respectively.

From Eq. (33) we see that $(d\rho/dz)^2$ can be approximated to a quartic polynomial for small values of E_e. Since we are interested in finding localized solutions for $\rho(z)$, with the asymptotic boundary condition $(d\rho/dz) \to 0$ and $\rho \to \rho_0$ as $z \to \pm\infty$, the quartic polynomial on the right hand side of Eq. (33) can be written in the form

$$\frac{1}{4}(d\rho/dz)^2 = (\rho-\rho_0)^2[L\rho^2 + M\rho + N]., \tag{34}$$

where the unknown quantities L, M, N are to be found consistently by equating the ρ^n terms ($n = 0$ to 4) on the right hand sides of Eqs. (33) and Eq. (34). Although this is a straightforward analysis, we give some details to show how the difference between the fractional and integer filling cases arises. We get

$$L = -2E_e;\ M = 2[E_e(1-\rho_0) - E_\omega);\ N = -2(E_e - E_\omega)\,\delta(\rho_0) - v^2, \tag{35}$$

where for convenience we use the notation $\delta(X) = 1(0)$ for $X = 0(X \neq 0)$.

We also get the following consistency condition:

$$(1-2\rho_0)(N+v^2)+2(1-\rho_0)^2[E_e(1-2\rho_0)-E_\omega] = 0 \tag{36}$$

From Eqs. (35), it is easy to see that for the integer filling cases $\rho_0 = 0$ and 1 , Eq. (36) is identically satisfied. In contrast, for the fractional filling case $0 < \rho_0 < 1$, since from Eq. (35), $N_F = -v^2$, Eq. (36), leads to the following *constraint* on E_ω

$$E_\omega = E_e(1-2\rho_0) = E_{\omega_F}. \tag{37}$$

This shows that for fractional filling, the two energies get related, so that the frequency takes on the *fixed* value

$$\hbar\omega_F/t = E_e(1-2\rho_0), \tag{38}$$

which is *dependent* on the effective energy of the HCB system. This is also in agreement with the expression found in the general features of the system discussed in the previous section (see discussion above Eq. (25)). In contrast, for integer filling $\rho_0 = 0, 1$, the frequency ω is *not* determined, and is hence an independently *variable* parameter.

Eq. (38) yields $\omega_F(\rho_0) = -\omega_F[(1-\rho_0)] = -\omega_F(\rho_h)$ showing the particle-hole symmetry explicitly, for fractional ρ_0. We remark that λ_0 can also be found consistently. Further, the analysis presented above is valid for small E_e positive, negative or zero (See above Eq. (34)). For the BH model parameters appearing in Eq. (1), this implies that V has to be an attractive interaction (i.e., $V > 0$).

We look for solutions

$$\rho(z) = \rho_0 + f(z). \tag{39}$$

Using this in Eq. (34), and substituting for L, M and N from (35) we see that for all ρ_0, we can write

$$\frac{1}{4}(df/dz)^2 = f^2[Af^2 + 2Bf + D], \tag{40}$$

where the constraint Eq. (37) applies for fractional filling only. By combining the results for fractional and integer filling densities, it is possible to write the following expressions for A, B and D which are valid for both types of fillings.

$$A = -2E_e;\ \ B = E_e(1-2\rho_0)\delta(\rho_0 - F) + (2E_e - E_\omega)\delta(\rho_0) - (2E_e + E_\omega)\delta(\rho_0 - 1), \tag{41}$$

where in B given above, F stands for any fractional value, $0 < F < 1$, and E_ω and E_e are defined in Eq. (31) and (24) respectively.

$$D = (c^2 - v^2) = c^2\gamma^2, \tag{42}$$

where c^2 is given by

$$c^2 = 2E_e\rho_0(1-\rho_0)+2(E_\omega-E_e)\delta(\rho_0)+2(-E_\omega-E_e)\delta(\rho_0-1), \tag{43}$$

and $\gamma^2 = (1 - \frac{v^2}{c^2})$. Equation (40) can be solved to give the following single functional form for the soliton solution :

$$f^\pm(z) = \frac{c^2\gamma^2}{\pm\sqrt{B^2 + 2E_e c^2\gamma^2}\cosh 2c\gamma z - B}. \tag{44}$$

Note that the soliton solution $\rho = \rho_0 + f$ obtained from the single profile (44) is valid for *both* fractional and integer filling backgrounds, although these two cases will possess different *physical* characteristics.

Due to the following particle-hole symmetry

$$f^\pm(\rho_0, \omega) = -f^\mp\big((1-\rho_0), -\omega\big) \tag{45}$$

it is sufficient to analyze solitons only for the fractional fillings $0 < \rho_0 \leq \frac{1}{2}$ and the integer filling $\rho_0 = 0$, from which those for $\frac{1}{2} < \rho_0 < 1$ and $\rho_0 = 1$ can be found.

Further, this soliton solution is valid for $E_e = 0$, as well as for both signs of E_e. As we will see, these various cases are quite distinct from each other.

VI. NP-TYPE AND P-TYPE SOLITONS

For a given ρ_0, the two solutions $f^\pm$ behave differently from each other. In the limit $\gamma \to 0$, Eq.(44) gives

$$f^\pm(v = c) = \frac{c^2\gamma^2}{\pm B[1 + c^2\gamma^2(E_e/B^2)\ + 2z^2] - B}. \tag{46}$$

This shows that f^- vanishes at its maximum speed $v = c$. Using $\rho = \rho_0 + f$, this leads to a density soliton which delo-

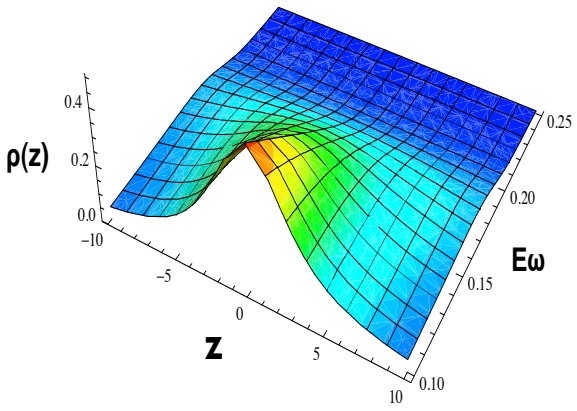

FIG. 2: Solitons propagating at speed $v/c = .999$ for $\rho_0 = 0$, $E_e = 0.1$, illustrating cross-over from P-type to NP-type with delocalization for $E_\omega \geq 0.2$.

calizes and hence is *nonpersistent* at its maximum speed. *Any soliton with this property will be termed NP-type soliton.*

Interestingly, at $v = c$, the solution f^+ tends to

$$f^+(v = c) = \frac{B}{[E_e + 2B^2 z^2]}. \tag{47}$$

Clearly, the corresponding density soliton survives and is *persistent* at its maximum speed. *Any soliton with this property will be termed P-type*. However, note that its localized profile vanishes algebraically (rather than exponentially) as $|z| \to \infty$. The density soliton arising from (47) is P-type and bright for $B > 0$, whereas it is dark for $B < 0$.

Further, the soliton becomes the following periodic soliton train for $v > c$:

$$f^+(v > c) = 2\frac{(v^2 - c^2)}{\sqrt{B^2 - 2E_e(v^2 - c^2)}\cos 2\sqrt{v^2 - c^2}z - B} \tag{48}$$

We will now discuss the characteristics of the soliton for various E_e.

A. $E_e = 0$

For this case, Eq. (34), the solution Eq. (44) is exact. Secondly, there are no sound waves, and *no* solutions exist for fractional filling backgrounds, $0 < \rho_0 < 1$. Hence we need to consider only integer fillings.

(i) $\rho_0 = 0$: Here, only bright solitons are possible. From Eqs. (43) and (41), we get $c^2 = 2E_\omega$, hence $\omega > 0$. Hence $B = -E_\omega$ is negative. Eq. (44) leads to

$$\rho(z) = \gamma^2 \mathrm{sech}^2\,(\mathrm{c}\,\gamma\,\mathrm{z}) \tag{49}$$

which is a *NP-type bright soliton*. Here, c is a function of ω. It is surprising that, the bright soliton (49) for the density ρ in the strongly *repulsive* HCB system with a zero background density, has a sech^2 form similar to that of the bright soliton for the weakly *attractive* GPE. However the detailed characteristics of these two solitons are quite distinct. For the latter, the traveling waves for the density and phase must travel with different speeds to support a bright soliton, in contrast with the former, where they travel with the same speed. In addition, its prefactor is not γ^2 but depends on the above two speeds.

We remark that bright solitons have been predicted and observed so far [2] only in weak, locally attractive systems. Our result (49) suggests that these should be looked for in strongly repulsive systems as well.

(ii) $\rho_0 = 1$: Here, from (43), the maximum speed is $c^2 = -2E_\omega$ showing that $\omega < 0$. Hence $B > 0$, yielding NP-type dark soliton of the form $\rho = 1 - \gamma^2 \mathrm{sech}^2\,(\mathrm{c}\,\gamma\,\mathrm{z})$. While the form of ρ is exactly the same as that of the dark soliton of the weakly repulsive GPE with background density $\rho_0 = 1$, its maximum speed is *not* the speed of sound.

B. $E_e > 0$

(i) Fractional filling:
This case, which corresponds to $0 < \rho_0 < 1$, is the only case discussed in our previous work [12]. We summarize the results for this case, in the interest of completeness as well as for comparison with the other cases to be discussed.

As seen from Eq. (43), the maximum speed of the soliton is the speed of sound, $c^2 = 2E_e\rho_0(1 - \rho_0)$ and the parameter $B = E_e(1 - 2\rho_0)$. (See Eq. (41).)

For $\rho_0 = 1/2$, since $B = 0$, the solutions Eq.(44) are mirror images of each other. Both of them lead to density solitons of NP-type, in the sense that they delocalize as $v \to c$. On the other hand, away from half-filling, for $0 < \rho_0 < 1/2$, we have $B > 0$, showing that $f^-(\rho_0)$ describes a NP-type dark soliton that dies as $v \to c$. In contrast, $f^+(\rho_0)$ leads to a bright soliton on a pedestal for the density, that survives at $v = c$, i.e., is P-type. Its exponentially decreasing profile transforms into the following algebraic profile:

$$f^+(v = c) = \frac{1 - 2\rho_0}{1 + 2E_e(1 - 2\rho_o)^2 z^2} \tag{50}$$

Summarizing, for $0 < \rho_0 < 1/2$ ($1/2 < \rho_0 < 1$) the dark (bright) soliton is NP-type and dies at the speed of

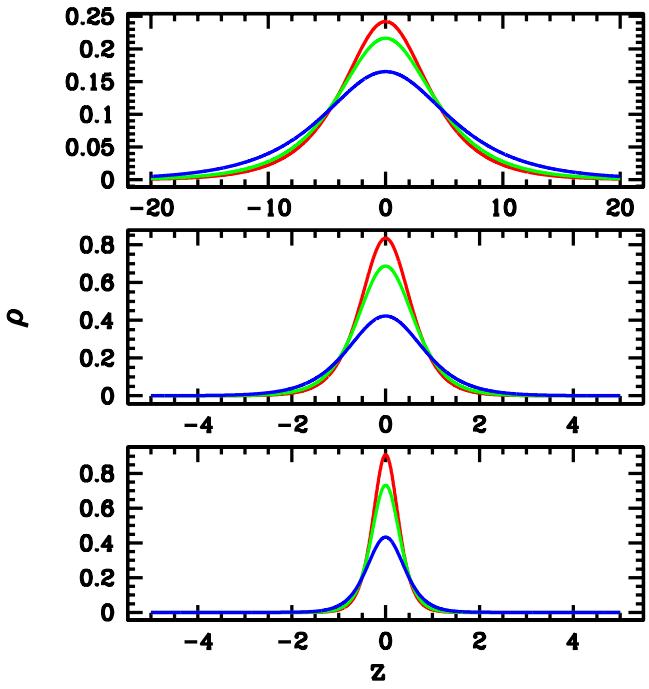

FIG. 3: For a fixed $E_e = 0.05$, the three curves in each plot illustrate bright soliton profiles for $\rho_0 = 0$, for $v/c = 0.25(red), 0.5(green), 0.75(blue)$. The upper plot is for $c = 0.158$, which is the maximum speed of sound possible for the fractional case, when $\rho_0 = 0.5$. The middle and the lower plots are for $c = 1$ and $c = 2$ respectively. We note that solitons in middle and lower plots have speeds 6.3 and 12.6 times faster than the speeds in the upper plot. Although $\rho_0 = 0$ solitons have no upper limit on their speed, the solitons profile become extremely narrow as c becomes large.

sound, whereas the bright (dark) soliton is of P- type which survives at the speed of sound, taking on an algebraic profile, and becomes a periodic soliton train at supersonic speeds.

(ii) Integer filling $\rho_0 = 0, 1$:

Before discussing this case in detail, in Fig. (1) we give the typical soliton profiles for density ρ and condensate density ρ^s found using Eq. (44), for two fractional filling cases as well as the integer filling case $\rho_0 = 0$, for comparison.

Cross-over from P-type to NP-type soliton:

There is an interesting manifestation in the limit $\rho_0 \to 0$ of the fractional filling case. In this limit, Eq. (43) implies $c \to 0$, so that the soliton becomes *static*, with a *fixed* frequency ω_0 such that $\hbar\omega_0/t = E_e$. But as soon as this limit is reached, the soliton solution corresponding to the integer filling $\rho_0 = 0$ takes over, with ω becoming a freely variable parameter. This is discussed below.

For $\rho_0 = 0$, firstly, we can have only bright solitons. From Eqs. (41) and (43), $B = (2E_e - E_\omega)$ and the maximum soliton speed is $c^2 = 2(E_\omega - E_e)$. In the $\rho_0 \to 0$ limit of the fractional case, since $\frac{\hbar\omega_F}{t} \to E_e$ (see Eq. (38)), this vanishes, and the soliton is indeed static. But ω is now a variable. For real c, we must have $E_\omega > E_e$. In addition, as we saw earlier, P-type, persistent bright solitons arise only for $B > 0$, i.e., $2E_e \geq E_\omega$.

Hence, we conclude that for $\rho_0 = 0$, P-type bright solitons for the density, that survive at the maximum soliton speed are supported for the range of frequencies $2E_e > E_\omega > E_e$. (Hence ω is positive.) However, a *cross-over* to NP-type occurs at a critical frequency $E_\omega = 2E_e$. In other words, for all $E_\omega \geq 2E_e$, the solitons are NP-type bright solitons that delocalize at the maximum soliton speed. This cross-over phenomenon is illustrated in Fig. (2).

At the critical frequency $E_\omega = 2E_e$, $B = 0$. Using this in Eq. (44), we find the NP-type bright soliton

$$\rho(z) = \gamma \mathrm{sech} 2\mathrm{c}\gamma\mathrm{z}, \tag{51}$$

which delocalizes for $v = c = \sqrt{2E_e}$. Note that both the above expression for the density, as well as that for the condensate density $\rho^s = \rho(1-\rho)$ are quite different from that of the well known bright GP soliton for GPE with attractive interaction.

For $\rho_0 = 1$, we have only dark solitons. Similar results can be obtained by using particle-hole symmetry.

For a *given* $E_e > 0$, our analysis shows that for the fractional filling case, the maximum soliton speed possible corresponds to half-filling, giving $c^2 = E_e/2$. In contrast, for integer filling, it appears as if the maximum speed $c^2 = 2(E_\omega - E_e)$ can keep on increasing as we increase ω. However, as shown in Fig. (3), the width of the soliton keeps decreasing with c. Hence, there will be an effective speed limit, below which the continuum solution we have used will remain valid.

C. $E_e < 0$

For $E_e \leq 0$, as is clear from Eq. (43), the system does not support solitons for fractional background density $\rho_0 = F$, but can support them for $\rho_0 = 0$ and 1.

(i) $\rho_0 = 0$: From (43), for c to be real, $E_\omega > -|E_e|$, and from (41), $B = [-2|E_e| - E_\omega]$. and the soliton behavior can be found as follows. For $B > 0$, we get $E_\omega < -2|E_e|$, which is not consistent with real c. Hence *no* soliton solutions can arise. For $B = 0$, the solution is purely imaginary, showing that again," *no* solitons possible. Finally, for $B < 0$, we see that *only* f^- solution in (44) is possible. This leads to a NP-type bright soliton solution for $E_\omega > -|E_e|$.

Hence, for $E_e < 0$, using particle-hole symmetry relations, it is easy to infer that for the background density $\rho_0 = 0$ ($\rho_0 = 1$), *NP-type bright solitons* (*NP-type dark solitons*)

exist for $E_\omega > -|E_e|$ ($E_\omega < |E_e|$), but P-type solitons do not arise at all.

This completes the discussion of soliton solutions of $\rho(z) = \rho_0 + f^{\pm}(z)$. We remark that the from $\rho(z)$, behavior of the solitons for the condensate density ρ^s can be found. It is also required for the discussion of magnetic solitons, as we will see.

VII. HCB SOLITONS MAPPED TO MAGNETIC SOLITONS IN HEISENBERG SPIN CHAINS

As pointed out in the beginning, the extended BH model Hamiltonian for HCB can be mapped to the classical XXZ ferromagnetic Heisenberg spin-$\frac{1}{2}$ Hamiltonian, on taking spin coherent state average of the Hamiltonian (15). The topic of magnetic solitons in Heisenberg chains that has been studied for over two decades [20, 21] continues to attract attention in recent times [22] as well. While the order parameter for BEC is the condensate density $\rho^s(z) = \rho(z)(1-\rho(z))$, the relevant order parameter for the spin Hamiltonian is $S^z(z)$, which can found from the HCB boson density $\rho(z)$ by using the identity $S^z = [(1/2) - \rho(z)]$. Thus all the soliton solutions for $\rho(z)$ which we found will also yield the corresponding magnetic soliton solutions for S^z.

In the last section, we found that in all cases, to obtain soliton solutions, it is *necessary* to have a purely time-dependent term $\omega\tau$ in (3). For a spin system, ω is just the precession frequency due to a corresponding "magnetic field" along the z-axis. Thus the *gauge-transformed* evolution equation (22) which led to solitons (44), also describes those for the continuum dynamics of the following dimensionless anisotropic Heisenberg spin Hamiltonian:

$$H_{eff}/t = -\sum_{j,a} \mathbf{S}_j \cdot \mathbf{S}_{j+a} + E_e \sum_{j,a} S^z_j S^z_{j+a} - E_\omega \sum_j S^z_j, \tag{52}$$

where E_e is the strength of the anisotropy energy (see Eq. (24)), and E_ω (see Eq. (31)) is the appropriate "magnetic field" along the z-axis, which would provide a physical origin for the above necessary spin precession.

(i) $E_e > 0$: Easy-plane anisotropic chain:

(a) Fractional background density $0 < \rho_0 < 1$: Recall that for this case, which now corresponds to $(-1/2) < S^z_0 < (1/2)$, this frequency ω_F is *fixed* and is given by $\hbar\omega_F/t = E_e(1-2\rho_0) = 2E_eS^z_0$. Eq. (52) yields

$$H_{eff}/t = -\sum_{j,a} \mathbf{S}_j \cdot \mathbf{S}_{j+a} + E_e \sum_{j,a} S^z_j S^z_{j+a} - \sum_j 2E_e\, S^z_0 S^z_j. \tag{53}$$

It is to be noted that unlike in usual spin chains, here the "external" magnetic field is not an independent variable, but depends on the anisotropy $E_e > 0$ and S^z_0.

Two competing terms appear: the easy plane anisotropy tends to make spins lie on XY plane, but the "magnetic field" tends to align spins along the z axis. Thus this magnetic field encodes the particle-hole imbalance $(1 - 2\rho_0))$ in the background.
For half-filling, since $\rho_0 = 1/2$, "magnetic field" vanishes. Hence there is no preferred direction about the z axis, and symmetric orientations above and below the easy plane are preferred by the excitations, yielding solitons that are *mirror images* of each other (see Fig.(1) (a)).

Away from half-filling, since $\rho_0 \neq 1/2$, the magnetic field is nonzero, and this symmetry is lost (see Fig. (1) (b). For fractional filling, $-1/2 < S^z_0 < 1/2$, we will get both NP-type and P-type magnetic solitons. These solitons we obtain for spin $S = \frac{1}{2}$ are similar to the A and B-type rotary wave solutions [21] found for magnetic solitons in spin S, easy-plane chains with a specific type of external field which depends on the anisotropy and the boundary condition on S^z. It is interesting that this type of spin Hamiltonian appears in a natural fashion in the extended BH model for HCB.

(b) Integer background density $\rho_0 = 0$ or 1, corresponding to $S^z_0 = 1/2$ or $-1/2$. Here, the precession frequency ω, which is *necessary* to create a soliton, is *not* fixed, and the spin Hamiltonian is given by (52), with the magnetic field term proportional to ω. Translating our results for the limit $\rho_0 \to 0$ we discussed for BEC, we find that it is possible to obtain P- type magnetic solitons for S^z that persist even at their maximum speed (which depends on ω) for a range of magnetic fields E_ω, beyond which they *cross-over* to NP-type magnetic solitons.

(ii) $E_e = 0$ and $E_e < 0$: Isotropic and Easy-axis anisotropic chain:
As is obvious, these can have only boundary conditions $S^z_0 = 1/2$ or $-1/2$, which correspond to integer filling backgrounds $\rho_0 = 0$ or 1. Hence ω is a variable parameter. However, in contrast to the easy plane case, these systems support only NP-type solitons for all ω.

In the existing literature [20, 21], magnetic soliton solutions for S^z in the classical isotropic chain ($E_e = 0$) as well as the easy plane ($E_e > 0$) and the easy axis ($E_e < 0$) anisotropic chains have been treated individually. As should be obvious, the advantage of our unified formulation is that we can now find all of them for various boundary conditions from a single functional form (44).

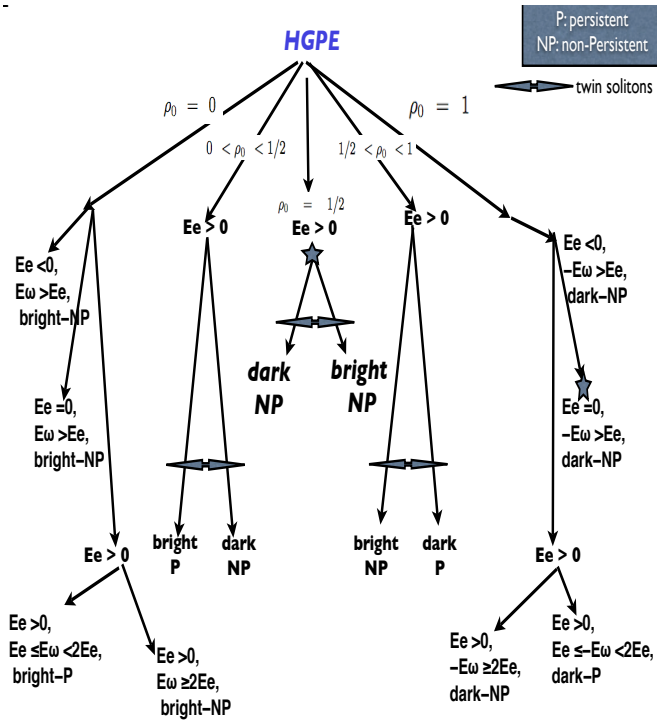

FIG. 4: Soliton Tree: Classifying the behavior of different types of density solitons of HCB for both fractional and integer background density ρ_0, with various E_e parameters. The star indicates that the corresponding soliton has a form similar to the GP soliton.

VIII. SUMMARY AND DISCUSSION

We have provided a unified formulation for finding solitary waves with various background densities, in the BEC of strongly repulsive bosons, described by a hard-core boson (HCB) system. Using an extended Bose-Hubbard (BH) model for HCB, which also includes nearest neighbor attractive interactions on the lattice, we show that in the continuum version, the condensate order parameter of this system satisfies Eq. (18), named by us as HGPE. Our comprehensive analysis also includes the GPE for weakly repulsive BEC, arising from the BH model of normal bosons. Interestingly, the GPE also emerges on neglecting certain nonlinear terms in the HGPE for low densities.

We find that while the *infinite* on-site repulsion condition $U/t \to \infty$, (i.e., $t << U$) for HCB in the BH model completely delocalizes the dark soliton in the GPE, (see Eq. (14)), the addition of a *finite* nn attractive potential $V \sim t$ which is much smaller than U, is sufficient to localize the dark soliton or even support bright solitons. As our results derived from (44) for the HGPE show, the behavior of the soliton depends on condensate boundary conditions as well as the sign and magnitude of E_e.

Commonality in the methodology to find solitons for both GPE and HGPE with various background densities, provides a simplified approach to understand these nonlinear modes in both cases. It also brings out certain universal aspects of the solutions, as well as certain distinguishing features.

We find it convenient to work with a *gauge-transformed* HGPE which has an inherent particle-hole symmetry. Solitary waves with amplitude and width expressed in terms of its maximum speed c and the corresponding γ (see Eqs. (14) and (44)) depict a kind of universality that emerges from our theoretical analysis which treats HGPE for various background densities as well as the GPE limit in equal footing. In addition to highlighting the universal aspects, we show that the solitons existing with and without background condensate density encode a fundamental distinction. Although in general, two competing energy scales E_e and E_ω appear in the HCB system, our systematic analysis shows that for the former these get related, giving a fixed frequency, whereas for the latter they remain independent parameters.

When the background condensate density is nonzero (i.e., fractional filling ρ_0) solitons exist only for $E_e > 0$, with the speed of sound as the maximum speed of the soliton. The soliton is characterized by its speed v alone, while its associated frequency ω_F is a constant, fixed by the background ρ_0 and the system parameters. For this case, the two species of condensate density solitons coexist: A dark soliton which is NP-type, and a novel P-type which persists even at sound speed, when it becomes fully bright.

When the background condensate density vanishes (i.e., integer filling ρ_0) the condensate density solitons exist for $E_e > 0$ as well as $E_e \leq 0$. There is no intrinsic speed of sound, nor a fixed frequency for these. The soliton is a function of v as well as its associated variable frequency ω. Further, the maximum soliton speed depends upon ω. For $E_e > 0$, the two species do not coexist. With an additional independent energy scale E_ω that emerges for the vanishing background density, the P-type bright solitons that survive even at the maximum speed $v = c$ exist only provided $E_e < E_\omega < 2E_e$. This shows that the energy E_ω (or "ground state" energy) associated with such a background should be at least E_e, to create even a static soliton excitation above the background. Energies higher than this make the soliton move, with the amplitude at its *maximum* (ω-dependent) speed $v = c$ remaining finite, showing its persistent nature. However, the amplitude for $v = c$ steadily decreases, till it vanishes at a *critical frequency* $E_{\omega_c} = 2E_e$, signaling a *cross-over* to the NP-type soliton for $E_\omega > 2E_e$.

A novel aspect of solitons in the HCB system described by HGPE is the possibility of creating very high speed localized modes in a system whose background has vanishing condensate density, by increasing the soliton frequency ω. The zero-background solitons for this strongly repulsive system can indeed be made to propagate with speeds that are much higher than the possible speeds in cases where solitons move in a background with a nonvanishing condensate density.

For $E_e \leq 0$, there is only one species of solitons for the condensate density. It is the NP -type bright soliton, for zero background condensate density.

Finally, by using the relationship $\rho(z) = \frac{1}{2} - S^z$, between HCB density and spin, we are also able to discuss the corresponding class of magnetic solitons in isotropic and anisotropic ferromagnetic spin chains in the presence of a magnetic field along the z-direction, in a unified fashion.

The "Soliton Tree" diagram given in Fig. (4) summarizes various possible solitary wave solutions for the density in the HCB system, providing a comprehensive picture of nonlinear modes in this strongly interacting bosonic system.

Soliton propagation has been studied experimentally in BEC using various techniques [6] such as the phase-imprinting method [1–3], which manipulates the initial BEC phase without affecting its density, the density-engineering method [4, 5] which creates an appropriate initial form for the density without affecting the BEC phase, and the quantum-state engineering method [3, 5] which manipulates both the density and the phase. We hope that our theoretical results will motivate experimental research on BEC solitons in the HCB system we have studied.

ACKNOWLEDGMENTS:
RB thanks the Department of Science and Technology, India, for financial support.

[1] S. Burger *et al.*, Phys. Rev. Lett. **83**, 5198 (1999); J. Denschlag *et al.*, Science **287**, 97 (2000)
[2] K. Strecker et al, Nature **417**, 150 (2002).
[3] C. Becker *et al*, Nature Phys. **4**, 496 (2008); S. Stellmer *et al* Phys. Rev. Lett. **101**, 120406 (2008).
[4] C. Dutton *et al*,Science **293**, 663 (2001); J. J. Chang, P. Engels and M. A. Hoefer, Phys. Rev. Lett, **101**, 170404 (2008).
[5] S. Burger *et al*, Phys. Rev. A **65**, 043611 (2002); L. D. Carr *et al*, Phys. Rev. A **63** 051601 (2001).
[6] D. J. Frantzskakis, J. Phys. A Math. Theor. **43**, 213001 (2010).
[7] Although strictly speaking, a soliton is a solitary wave that retains its characteristics intact even on collision, we shall use "soliton" to denote a "solitary wave", in this paper.
[8] C. J. Pethick and H. Smith *Bose-Einstein condensation in dilute gases* (Cambridge University Press, Cambridge, 2001)
[9] See, for instance, L. Pitaevskii and S. Stringari, *Bose-Einstein Condensation* (Oxford University Press, Oxford, 2003).
[10] See, for example, T. Dauxois and M. Peyrard, *Physics of Solitons* (Cambridge University Press, Cambridge, 2006), and references therein.
[11] R.V. Mishmash and L. D. Carr, Phys. Rev. Lett. **103**, 140403 (2009); R. V. Mishmash *et al*, Phys. Rev. A **80**, 053612 (2009).
[12] R. Balakrishnan, I.I. Satija and C. W. Clark, Phys. Rev. Lett. **103**, 230403 (2009); R. Balakrishnan and I. I. Satija, Pramana **77**, 929 (2011).
[13] See, for example, S. Sachdev, *Quantum Phase Transitions* (Cambridge University Press,Cambridge, 1999).
[14] J. M. Radcliffe, J. Phys. A **4** 313 (1971).
[15] I. I. Satija and R. Balakrishnan, Phys. Lett. A **375**, 517 (2011).
[16] W. Reinhardt, I. I. Satija, B. Robbins and C. W. Clark, arXiv: quant-phys 1102.4042.
[17] Chester P. Rubbo, Indubala I. Satija, William P. Reinhardt, Radha Balakrishnan,Ana Maria Rey, and Salvatore R. Manmana , Phys. Rev. A **85**, 053617 (2012)
[18] J. H. Denschlag *et al*, J. Phys. B **35**, 3095 (2002); S. Peil *et al*, Phys. Rev. A **67**, 051603 (2003).
[19] J. S. Langer, Phys. Rev. **167**, 183 (1968).)
[20] H. J. Mikeska and M. Steiner, Advances in Physics **40**, 191 (1990).
[21] A. M. Kosevich, B. A. Ivanov and A.S. Kovalev, Phys. Rep. **194**, 117 (1990).
[22] J. Lu *et al* Phys. Rev. E **79**, 016606 (2009); M. A. Hoefer, T. J. Silva and M. W. Keller, Phys Rev B, **82**, 054432 (2010).